



COMBINED LASER-MICROPLASMA CLADDING WITH POWDERS OF Ni-Cr-B-Si SYSTEM ALLOYS

Yu.S. BORISOV, V.Yu. KHASKIN, S.G. VOJNAROVICH, A.N. KISLITSA, A.Yu. TUNIK, L.I. ADEEVA, E.K. KUZMICH-YANCHUK, A.V. BERNATSKY and A.V. SIORA

E.O. Paton Electric Welding Institute, NASU, Kiev, Ukraine

Structural features of deposited layers produced by the combined laser-microplasma method using powders of the Ni-Cr-B-Si system alloys were investigated. Technological advantages and drawbacks of a combination of laser cladding and microplasma spraying were determined. It was shown that the developed combined laser-microplasma method allows improving the quality of the deposited layers by preserving the key advantages characteristic of the laser powder cladding process.

Keywords: *combined laser-microplasma cladding, self-fluxing nickel alloy, structure, phase composition, hardness, wear resistance*

Different thermal spraying methods, such as flame, plasma and detonation ones, are applied to deposit coatings of alloys of the Ni-Cr-B-Si system. Spraying and melting can be performed in one (gas powder cladding) or two successive stages (spraying with subsequent melting of the sprayed layer). The sprayed NiCrBSi coatings preserve the main properties of the NiCrBSi alloy (wear and corrosion resistance), but lack the high adhesion strength (normally, less than 35–40 MPa). After melting the strength of adhesion of the NiCrBSi coating layer to the substrate grows to 70–75 MPa [1].

For a number of industrial problems it is desirable that the adhesion strength value be as close as possible to strength of the base metal. In this connection, of an increasing interest now is the process of laser melting of coatings. Advantages of this process include thermal locality and minimal effect on the base metal, as well as small (5–20 μm) size of the transition zone, which minimises penetration of the base metal into the deposited one and favours refining of structure of the material, this resulting in improvement of mechanical properties. However, shrinkage cracks may form in laser melting as a result of dramatically heterogeneous heating, especially of coatings more than 0.5 mm thick, as well as subsequent cooling [2, 3].

It is noted in studies [4–6] that drawbacks characteristic of laser melting can be eliminated by combining plasma and laser heating. One of such processes, which integrates advantages of laser cladding and microplasma spraying, is combined laser-microplasma cladding (CLMPC) [7].

It allows avoidance of drawbacks characteristic of laser cladding (formation of internal pores and microcracks), preparation of the workpiece surface directly during the process of deposition of a material, and fusion of the deposited layers with the base metal.

The purpose of this study was to investigate structural peculiarities of the layers deposited with powders of the Ni-Cr-B-Si system alloys (PG-12N-01 and PG-12N-02) by the CLMPC process, as well as to define technological advantages of combining the laser cladding and microplasma spraying processes.

Investigation procedure. Layers 0.3–1.2 mm thick were deposited on substrates of steels St3 and 38KhN3MFA by the CLMPC method using self-fluxing alloy powders (PG-12N-01 and PG-12N-02). Structure, phase composition and properties of the layers were investigated. An integrated procedure comprising metallography (microscope «Neophot-32» with digital photography attachment), durometric analysis (LECO hardness meter M-400 with loads of 0.25, 0.5 and 1 N) and X-ray phase analysis in monochromatic CuK_α -radiation by using diffractometer DRON-UM1 was applied for investigation of the resulting deposited layers. Graphite single crystal placed on a path of the diffracted beam was used as a monochromator. Diffraction patterns were made by the step scan method in the $20^\circ < 2\theta < 90^\circ$ angle range. The scan step was 0.05° , and the time of exposure at a point was 3–7 s. The data of the diffractometry experiment were processed by using software PowderCell 2.4 for full-profile analysis of X-ray spectra of a mixture of polycrystalline phase components.

Cracking index α the value of which was determined in percent was introduced to compare



the quantity of cracks in clad specimens. The absence of cracks in the deposited layer was taken as zero, and the network of cracks with a pitch of 1 mm was taken as 100 %. The investigations showed that this index can be estimated from formula $\alpha = 3/L$, where L is the distance between the cracks, mm.

Investigation of wear resistance of the deposited layers was carried out by using friction machine 2070 SMT-1 by the disk–pin method without lubrication. Before the investigation the 40 mm diameter specimens were polished to surface finish $R_a = 1.6 \mu\text{m}$. Material of the mating body was steel 45 heat treated to hardness HRC 55. Prior to the tests, the surfaces were subjected to running-in, the presence of which was fixed from stabilisation of the friction moment in a pair. Relative wear resistance was determined from the loss of weight at sliding speeds of 1.3 m/s in a mode of stepwise loading, the test time at each step being 15 s, and load being 0.2 kN. Wear resistance of the clad specimens compared to that of the base metal was determined by using the in-house friction machine according to the cylinder–pin scheme by the dry friction method. As this machine is a non-standard development, the results obtained by using it were regarded as relative. A specimen of steel 38KhN3MFA after volumetric (furnace) hardening and heat treatment, having hardness HRC 43–44, was chosen as the reference one. Wear of the specimens measured from a change in weight (in grams) was compared with that of the reference specimen. The time of friction was increased to improve accuracy of the measurement results. The mating body was made from hard alloy T15 or steel 45 hardened to HRC 50–55. The specific pressure was set within 11–12 MPa, the rotation speed for a test specimen was 50–1600 rpm, and the linear friction speeds were 0.4–15.0 m/s. In all the cases the specimens were weighed before and after the friction tests by using analytical balance VPR-200 within 0.0005 g.

Materials, equipment and principle of operation of the devices. Self-fluxing nickel alloy powders PG-12N-01 and PG-12N-02 with a particle size of 40–100 μm (TU 48-19-383–84), the chemical compositions of which is given in Table 1, were used as materials for cladding. The powders produced by atomisation in inert gas had particles with a regular round shape, close to the spherical one. The fractional composition of the powders was -40 – $+100 \mu\text{m}$. Hardness of

Table 1. Chemical composition of nickel alloy powders (Ni – base), wt.%

Powder grade	Cr	B	Si	Fe	C
PG-12N-01	8–14	1.7–2.8	1.2–3.2	2–5	0.3–0.6
PG-12N-02	10–16	2.0–4.0	3.0–5.0	3–6	0.4–0.8

the PG-12N-01 powder was HRC 36–45, and $T_{\text{melt}} = 1080 \text{ }^\circ\text{C}$. Hardness of the PG-12N-02 powder was HRC 46–55, and $T_{\text{melt}} = 1050 \text{ }^\circ\text{C}$.

CO_2 -laser TR-100 (Rofin-Sinar, Germany) with a power of up to 10 kW was used as a laser radiation source. Radiation of this laser with a power of 2, 3 and 4 kW, combined with the microplasma jet with a power of up to 1.5 kW, was used in the experiments.

The MPN-004 system with the MP-04 microplasmatron developed by the E.O. Paton Electric Welding Institute of the NAS of Ukraine was used to form the microplasma jet (design of the microplasmatron is covered by the Ukrainian patent «Plasmatron for spraying of coatings» No. 2002076032) UA, B23K10/00.

Design and operating parameters of the microplasmatron provide formation of the laminar plasma jet (Reynolds criterion is 0.10–0.55). According to this criterion, the microplasma spraying process is characterised [8] by:

- low thermal power, this making it possible to decrease heating of the substrate and deposit coatings on small-size and thin-walled pieces without substantial local overheating and buckling;
- low level of noise in spraying with the laminar plasma jet, which is no more than 30–50 dB, this allowing avoidance of cumbersome protection chambers;
- small size of the spraying spot (1–5 mm) at a small diameter of the nozzle equal to 1–2 mm.

The latter parameter is the key one for implementation of the laser-microplasma cladding process, as it provides adequacy of the geometric size of the spraying spot to the focal spot of the laser. Therefore, with a spraying spot of about 5 mm, it can be completely overlapped by the focal spot of the laser, the thermal power density in the spot being sufficient for remelting of the sprayed layer and its fusion with the substrate.

Flow diagram of the cladding process is shown in Figure 1. A specimen (plate) was mounted on a working frame approximately at equal angles to axes of the laser beam and plasma jet. The laser beam was fed vertically from above. The plasma jet transporting the cladding powder was directed to the focusing spot normal to the laser beam. The laser beam and microplasma jet action

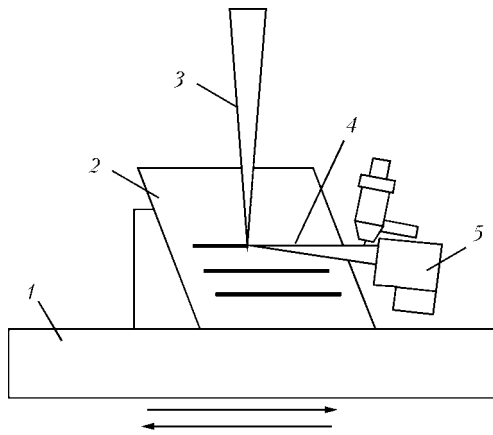


Figure 1. Flow diagram of the combined laser-microplasma cladding process: 1 – frame; 2 – specimen; 3 – laser beam; 4 – plasma jet; 5 – microplasmatron

zones were combined to form the common zone, the frame with the specimen mounted on it being moved relative to this common zone. Additional scanning by using a scanator (Figure 2) was used to smooth down the surface of the deposited layer.

The principle of operation of this device is as follows: DC motor 3 (see Figure 2, *b*), the rotation frequency of which is adjustable within 10–200 rpm, imparts the torque moment to eccentric 2, whose axis is shifted relative to the motor axis. The eccentric engages holder 1, thus forcing it to oscillate relative to the semi-axes. The lens fixed in the holder oscillates together with it. This leads to periodic deflections of the radiation focusing axis from the vertical position, which in turn shifts position of the focal spot. As a result, the laser beam focusing spot on a work-piece starts oscillating at a certain frequency depending on the rotation frequency of motor 3. The amplitude of such oscillations depends on the value of eccentricity, which is set by using

eccentric 2. Return of the holder back to the initial position is provided by spring 5, which is constantly kept in the compressed state. The entire structure is mounted on swinging bracket 4, which makes it possible to arbitrarily select direction of the oscillations relative to the laser treatment direction. This allows both transverse and longitudinal oscillations of the beam.

Experimental. To determine dependence of height h (mm) of the deposited layer on the process parameters, initially the process was performed by depositing single beads on a plate of steel St3 ($\delta = 8$ mm). The following parameters were chosen as the variable ones: laser radiation power P_{laser} (kW), energy input E (J/mm), and specimen movement speed v (m/h). Powder consumption G_p during the experiments was varied within 0.1–0.2 g/s. Other process parameters were kept constant: diameter of the spot of the beam focused on the specimen surface $d_{\text{sp}} = 5$ –6 mm, plasmatron current $I = 43$ A, voltage $U = 30$ V, plasma gas (argon) flow rate $Q = 80$ l/h, and shielding gas (argon) flow rate $Q_{\text{sh}} = 240$ l/h. To optimise the value of overlapping of the beads (according to the criterion of roughness of the resulting coating on a similar plate), several beads were deposited by overlapping 10–50 % of their width.

Decrease in height of the deposited bead with increase in power of the laser beam (Table 2, specimen 1) is related to a burn-off loss of part of the cladding material, as well as to overheating of the base metal and dissolution of part of the deposited bead material in it. Increase in height of the bead (Table 2, specimen 5) is attributable to the noted instability in feeding the powder.

Results and discussions. Based on the experimental results, the mode corresponding to speci-

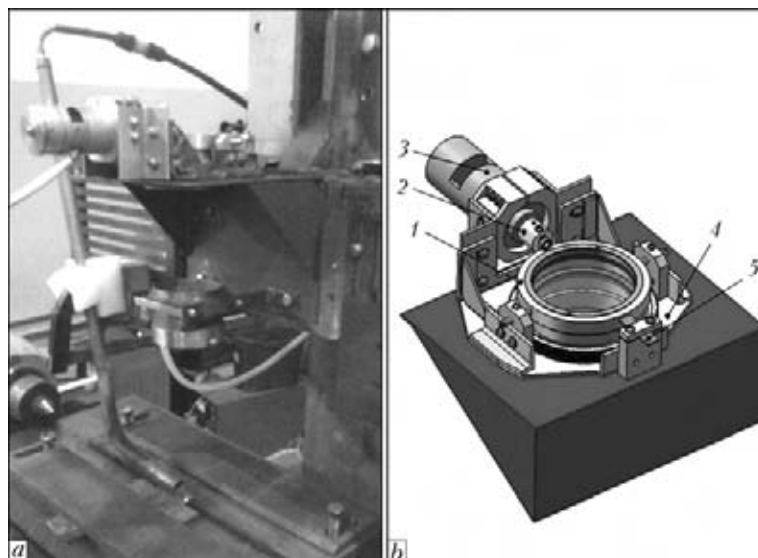
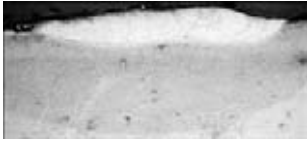
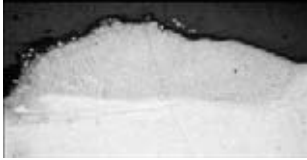

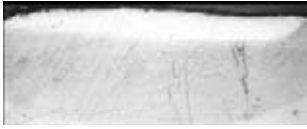





Figure 2. Appearance (*a*) and schematic of structure of the laser radiation scanator (for designations see the text)



Table 2. Effect of power and speed of movement of a specimen in CLMPC on height and quality of the bead deposited with powders PG-12N-02

Specimen number	P_{laser} , kW	v , m/h	E , J/mm	Microstructure, $\times 20$	h , mm	Note
1	4	30	635		0.4	Presence of microcracks
2	3	6.5	2380		1.2	Bead is non-uniform in height
3	3	10	1545		0.8	Bead is uniform
4	3	20	770		0.6	Same
5	3	30	520		1.0	»
6	2	10	1185		0.3	Bead is non-uniform in profile
7	2	20	590		–	Bead is not formed

men 4, which provided the defect-free layers at a comparatively low energy input, was chosen to implement the process of laser-microplasma cladding of steels with powders of the Ni–Cr–B–Si system alloys. Decrease in energy input led to formation of such a defect as microcracks (see Table 2, specimens 1 and 5). Further investigations showed that with increase in the powder consumption to $G_p = 0.5\text{--}0.8$ g/s the speed of movement can be increased to 60 m/h, other parameters being kept unchanged. This will provide the deposited beads with the geometry similar to that described in Table 2, along with decrease in the HAZ. In addition, it was established that the acceptable roughness of the deposited layers (about $R_a = 200\text{--}300$ μm) occurs at the coefficient of overlapping of the beads equal to $K_{\text{ov}} = 25\text{--}30$ %. It means that at a bead width of

6 mm the transverse movement of a specimen for deposition of each next bead will be not less than 4 mm. Also, it was established that the optimal parameters for laser-microplasma cladding can be provided at an energy input ranging from 500 to 800 J/mm. For comparison, it should be noted that in laser powder cladding the energy input is 120–250 J/mm [9]. This shows that overheating of the deposited layers and increase in size of HAZ should take place in the case of combined cladding, in contrast to laser cladding.

Overheating of the layers deposited by the laser-microplasma method leads to some decrease in their hardness. The higher the energy input in the process and, hence, the higher the temperature in the working zone, the bigger this decrease is. This is explained by the fact that in plasma spraying of self-fluxing alloys at a temperature

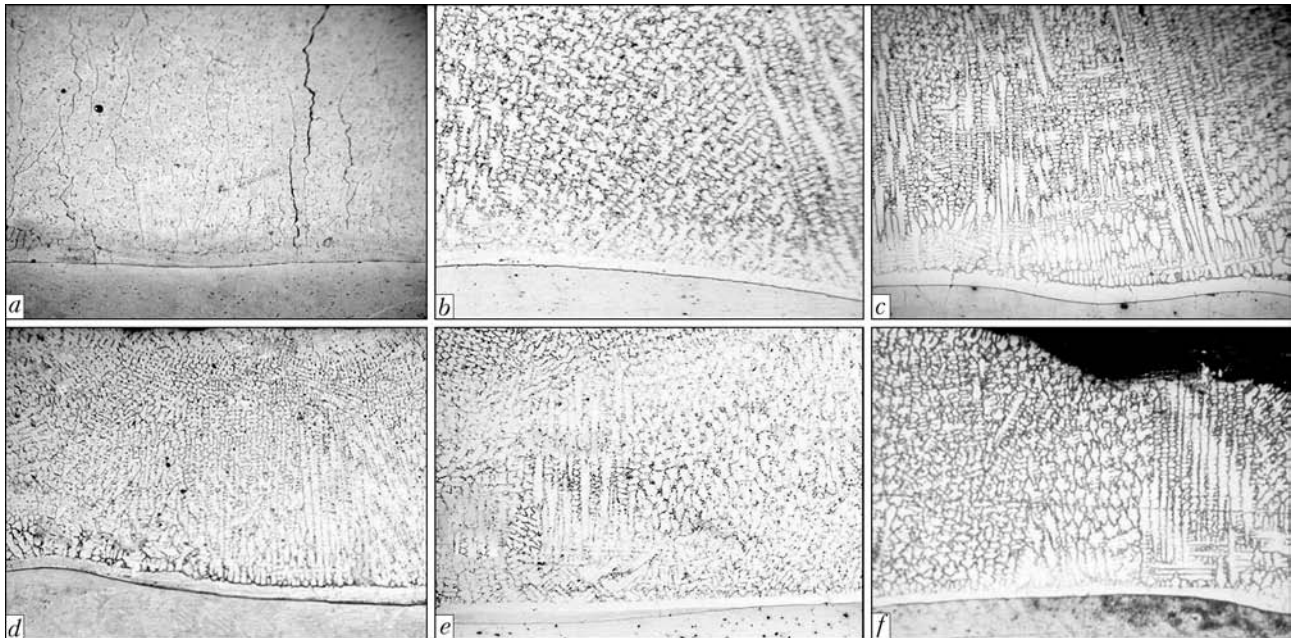


Figure 3. Microstructures ($\times 100$) of the layers deposited by the CLMPC method using powder PG-12N-02: *a-f* – specimens 1–6, respectively, from Table 2

close to their melting temperature the burn-off (oxidation) of boron takes place to form B_2O_3 . According to the data of study [10], at a temperature of $2000\text{ }^\circ\text{C}$ the content of B_2O_3 in the oxide film within the process zone amounts to 81 at.%. Under the combined laser-microplasma process conditions the temperature of the working zone is higher than in plasma spraying, this intensifying burning-off of boron.

As shown by the experiments, in deposition of the layers not less than 0.6 mm high at an energy input ranging from 300 to 400 J/mm the decrease in hardness is minimal. The layers deposited at the above energy inputs have hardness that corresponds to the certificate hardness of the applied cladding alloys. Investigations of the layers produced by the CLMPC method showed that on all the specimens the deposited layers have a sufficiently fine cast structure. Moreover, formation of columnar dendrites of metal, which grew in a direction of heat removal from the zone of fusion with the base metal, takes place in the lower part of the deposited layers. In the upper part of the deposited layers, the columnar dendrites propagate, as a rule, into the zone of finer equiaxed crystals, which is accompanied by some increase in microhardness. The microhardness of the layers deposited at the specimen movement speeds of up to 30 m/h in most cases amounts to about 3000 MPa.

Examinations of structures of the deposited specimens showed the following. Specimen 1 (see Table 2 and Figure 3, *a*) differed from the rest of the specimens in the presence of structural defects, such as transverse cracks in the cast struc-

ture that propagated along the boundaries of dendrites in the deposited metal. HAZ in the base metal was rather big. Its width was 2.5 times bigger than cladding thickness. Specimens 2–4 (see Figure 3, *b-d*) had no cracks and no separations from the substrate. Microcracks similar to those observed in specimen 1 were detected in specimen 5, which can be explained by close energy inputs in cladding of these specimens. Specimens 6 and 7 sprayed at a lower power of the laser were characterised by formation of a lower-quality bead. In all the specimens the deposited metal had the cast dendritic structure, transforming into the fine-crystalline one in the upper part. Interlayers consisting of nickel borides Ni_3B and nickel silicides Ni_2Si and, probably, their eutectics with $\gamma-Ni$, as well as chromium carbides $Cr_{23}C_6$ and Cr_7C_3 , were located along the boundaries of light dendrites, which were $\gamma-Ni$ based solid solution.

The feature in common to the specimens is that the dendritic structure of the cladding near the zone of fusion with the base metal was free from inclusion. Structure of the fusion region (white strip) consisted of $\gamma-Ni$ solid solution and had a decreased hardness, 25 % lower, on the average, than hardness of the cladding. The region located below the fusion zone (HAZ) can be subdivided into two parts as to its depth: a region adjoining the fusion zone, having hardness of 2590–3260 MPa, and a region located below, which adjoins the base metal and has hardness of 1580–1940 MPa. Microhardness of the base metal was 2100–2310 MPa, on the average. Presumably, the presence of the HAZ metal regions

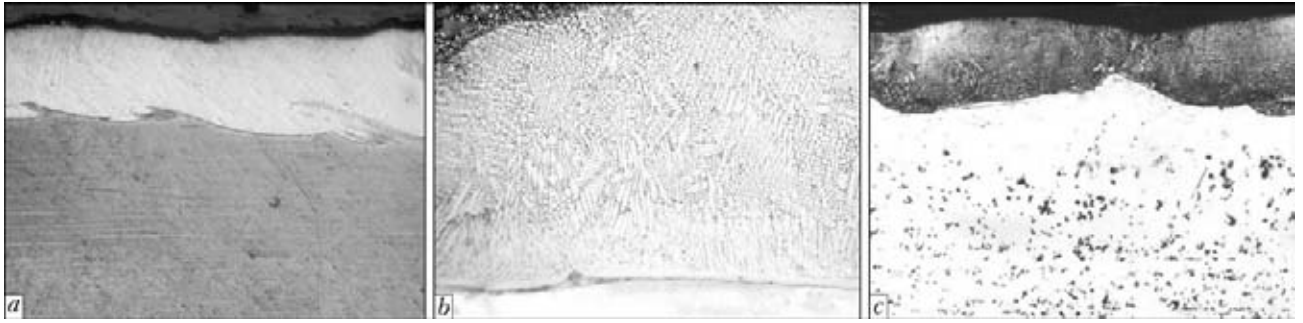


Figure 4. Microstructures of the layers deposited by the CLMPC method using powder PG-12N-02 at a process speed of 20 (*a*, *b*) and 50 (*c*) m/h with transverse scanning of the laser beam (*a* – $\times 25$; *b* – $\times 100$) and without it (*c* – $\times 32$)

with a different hardness can be explained by a diffusion redistribution of elements. Probably, such alloying elements as carbon, boron and silicon propagated from the deposited layer into that part of HAZ which adjoins the transition part. Moreover, it is likely that carbon from the lower part of HAZ redistributed to the upper part. Size and hardness of the cladding regions and metal depend on the combination of parameters of the laser and microplasma processes, consumption of the additive powder and speed of movement of a specimen in CLMPC.

The experiments showed that increase in the laser beam focusing spot up to values of $d_{sp} = 5-6$ mm leads to the need to use a substantial power of laser radiation (about 3 kW). To decrease the latter and reduce roughness of the surface of the layer, the laser beam was additionally scanned across the cladding with amplitude of 2 mm and frequency of about 20 Hz. The beam was scanned by using a scanator (see Figure 2).

Adding of scanning of the laser beam across the CLMPC direction allowed diameter of the spot focused on the surface treated to be decreased to 4 mm, and laser radiation power to be reduced to 2 kW. Other process parameters were kept constant. Adding of scanning of the laser beam reduced the sensitivity of the deposited layers to cracking. The general trends in formation of structure in these layers remained unchanged (Figure 4, *a*, *b*).

Quality of the resulting layers also depends on the consumption of the additive powder. For example, the CLMPC process without scanning of the laser beam, at the PG-12N-02 powder consumption of $G_p = 1.0-1.2$ g/s, allowed depositing the sound layers 0.5–0.6 mm high at a speed of 50 m/h and at radiation power $P = 3$ kW. In this case the size of HAZ was approximately equal to height of the deposited coating (Figure 4, *c*). Therefore, the indicated consumption of the additive powder materials for CLMPC is 0.8–1.2 g/s.

The results obtained in the above experiments were compared with the results of cladding of

similar materials performed by the laser powder cladding method developed at the E.O. Paton Electric Welding Institute [9]. It turned out that they were rather close in value of irregularities (roughness) and appearance of the clad surfaces. The main difference consisted in sticking of an insignificant quantity of the powder material to the surface in CLMPC.

It was found that the layers of the Ni–Cr–B–Si system alloys deposited by the laser method had a cracking index of about 40–60 % ($\alpha = 0.4-0.6$), whereas the combined cladding allowed decreasing this index from 10–20 % ($\alpha = 0.1-0.2$) to a complete elimination of microcracks.

Both standard friction machine 2070 SMT-1 and in-house friction machine were used to determine wear resistance of the deposited layers.

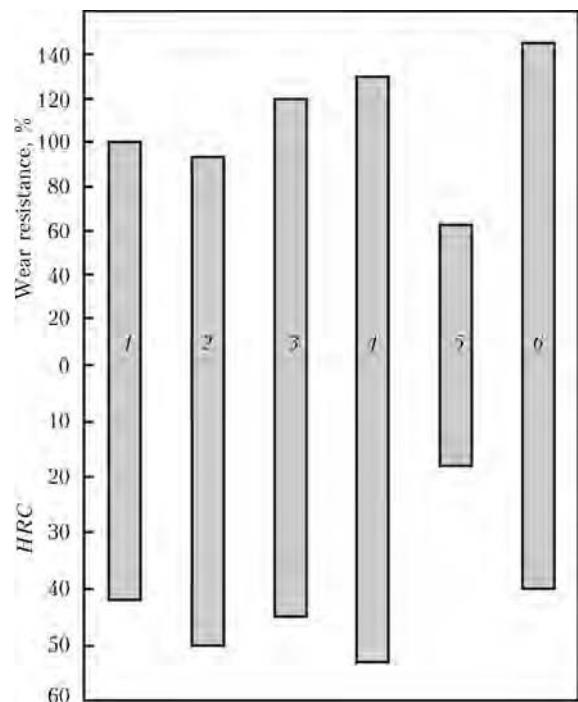


Figure 5. Comparison of wear resistance and hardness *HRC* of Ni–Cr–B–Si system alloys deposited by different methods with those of steel 38KhN3MFA in dry friction: 1 – 38KhN3MFA; 2 – plasma spraying with powder PG-12N-02; 3, 4 – laser cladding with PG-12N-01 and PG-12N-02, respectively; 5, 6 – combined deposition of layers with PG-12N-01 and PG-12N-02



Wear resistance in dry sliding friction was determined in percent, by taking wear resistance of steel 38KhN3MFA with hardness *HRC* 42–43 as 100 %. It was established as result that the wear resistance values in CLMPC can be superior to those characteristic of laser cladding. However, in a case of failure to comply with the thermal conditions, i.e. overheating of specimens at low cladding speeds, the value of wear resistance may decrease to a substantial degree because of weakening of the hard phases. An example of such decrease in wear resistance of metal deposited with powder PG-12N-01 is shown in Figure 5. There this indicator decreased almost to 60 % relative to the same indicator for steel 38KhN3MFA.

CONCLUSIONS

1. The efficiency of applying CLMPC is determined by decrease in the quantity of microcracks in the deposited layers. For instance, the layers of Ni–Cr–B–Si system alloys (PG-12N-01 and PG-12N-02) deposited by the laser method had a cracking index of about 40–60 %, whereas combined cladding of the same alloys allowed decreasing this index from 10–20 % to complete elimination of microcracks.

2. Comparative dry friction tests of specimens of the base metal (steel 38KhN3MFA, whose wear resistance was taken as 100 %) and specimens deposited with the same Ni–Cr–B–Si system alloys showed the possibility of providing wear resistance of an order of 120–130 % in laser powder cladding, and more than 140 % in CLMPC.

3. Along with the above advantages, CLMPC has certain drawbacks compared to laser cladding. The key drawbacks include increase in size of HAZ in the base metal, decrease in hardness of the deposited layers as a result of weakening of metal (burn-off loss (oxidation) of boron and, hence, decrease in the content of the boride phases, as well as coagulation of particles of the

strengthening carbide and silicide phases). The cause is increase in temperature of the working zone due to a substantial growth of the process energy input (to 500–800 J/mm), compared to laser cladding (normally 120–250 J/mm), which is required to achieve the optimal parameters.

4. Further investigations on elimination of the said drawbacks will show expediency of applying laser-microplasma cladding for deposition of wear-resistant coatings both in manufacture and in repair of parts of the shaft type operating in friction pairs (e.g. components of sleeve assembly of internal combustion engines, and running gear of motor and railway transport).

1. Borisov, Yu.S., Kharlamov, Yu.A., Sidorenko, S.L. et al. (1987) *Thermal spray coatings from powder materials*: Refer. Book. Kiev: Naukova Dumka.
2. Grigoriants, A.G., Safonov, A.N., Shibaev, V.V. (1982) Production of wear-resistant chrome-nickel and chrome-boron-nickel coatings by using laser radiation. *Izvestiya Vuzov. Mashinostroenie*, **3**, 87–92.
3. Safonov, A.N., Grigoriants, A.G., Shibaev, V.V. et al. (1984) Investigation of crack formation in laser cladding of chrome-boron-nickel powdered alloys. *Ibid.*, **12**, 64–68.
4. Dilthey, U., Wieschemann, A. (2000) Prospects by combining and coupling laser beam and arc welding processes. *Rivista Italiana della Saldatura*, **52**(6), 749–759.
5. Coddet, C., Montaron, G., Marchione, T. et al. (1998) Surface preparation and thermal spray in a single step: the PROTAL process. In: *Proc. of 15th ITSC* (Nice, France), Vol. 1, 1321–1325.
6. Krivtsun, I.V. (2002) *Combined laser-arc processes of materials treatment and devices for their realization*: Syn. of Thesis for Dr. of Techn. Sci. Degree. Kiev: PWI.
7. Shelyagin, V.D., Krivtsun, I.V., Borisov, Yu.S. et al. (2006) Laser-arc and laser-plasma welding and coating technologies. *Svarka v Sibiri*, **1**, 32–36.
8. Borisov, Yu.S., Vojnarovich, S.G., Bobrik, V.G. et al. (2000) Microplasma spraying of bioceramic coatings. *The Paton Welding J.*, **12**, 63–67.
9. Velichko, O.A., Avramchenko, P.F., Molchan, I.V. et al. (1990) Laser powder cladding of cylindrical parts. *Avtomatich. Svarka*, **1**, 59–65.
10. Gershenzon, S.M., Borisov, Yu.S., Razikov, M.I. et al. (1978) Interaction of self-fluxing nickel alloys with oxygen. *Svarochn. Proizvodstvo*, **1**, 9–11.